Tsunami fragility curves of a RC structure through different analytical methods

C. Petrone[1], T. Rossetto, I. Eames
EPICentre, University College London, London, United Kingdom

K. Goda
University of Bristol, Bristol, United Kingdom

ABSTRACT

Recent tsunami events have stimulated research activity into tsunami fragility functions which have been largely based on empirical data. However, empirical fragility functions are biased because the influence of earthquake and tsunami damage are difficult to separate. We develop a new theoretical framework to assess the structural performance of a building due to tsunami inundation by drawing on recent experimental and theoretical progress at UCL on building. Different nonlinear static analyses, i.e. constant-height pushover (CHPO) and variable-height pushover (VHPO), are compared with nonlinear dynamic analysis in assessing the fragility curves of a case study structure for a set of realistic tsunami wave traces. The results of VHPO provide a good prediction of collapse fragility curves obtained from the dynamic analysis under a wide range of tsunami time-histories. On the other hand, CHPO provides a larger, i.e. about 10% in median value, fragility in case global failure is considered and a smaller fragility for local shear failure. On the basis of these results, it is recommended that VHPO be used in future fragility analysis of buildings subjected to tsunami.

Keywords: tsunami engineering, fragility curve, analysis methodology, pushover analysis, time-history analysis, tsunami force, tsunami simulation

INTRODUCTION

Recent tsunami events (e.g. 2004 Indian Ocean tsunami and 2011 Great East Japan tsunami) have caused numerous deaths and widespread damage. The observed impacts from tsunami can only be reduced through the development of comprehensive mitigation plans based on tsunami impact scenarios and risk assessments. An important component in the evaluation of tsunami impact or risk is the estimation of building fragility due to tsunami onshore flow. This has recently been recognised by researchers worldwide (Dias et al. 2009; Suppasri et al. 2012; Charvet et al. 2014). To date the majority of this research has focussed on the development of fragility functions based on observational post-tsunami damage data, in particular after the 2004 Indian Ocean tsunami (e.g. (Koshimura et al. 2009; Suppasri et al. 2011)) and the 2011 Japan tsunami (e.g.(Charvet et al. 2014)). Empirical tsunami fragility functions are by their nature specific to the event represented in the post-event damage data as well as the local building stock, and is influenced by the absence of locally recorded tsunami intensity measures (IMs). Tsunami inundation depths can be obtained from the inspection of water marks on standing buildings, whereas other IMs, such as flow velocity, is difficult to assess after the event. It is important to recognise that the building damage observation data have been affected by both earthquake and tsunami loads, and implicitly include the response of buildings to the combined hazards. As post-tsunami

---

[1] Corresponding Author: C. Petrone, EPICentre, University College London, London, United Kingdom, c.petrone@ucl.ac.uk

reconnaissance cannot distinguish between damage from the two hazards, it is difficult to determine whether preceding damage due to the earthquake has affected structural response to the tsunami inundation. The assessment of structural performance through numerical analyses is therefore essential to overcome the mentioned limitations of empirical fragility functions. Analytical fragility functions can also be used together with empirical assessments to provide a deeper understanding of structural behaviour under tsunami actions.

Very few studies on tsunami fragility of structures with analytical method are available in the literature. All the existing tsunami analytical fragility approaches (Park et al. 2012; Foytong et al. 2015; Nanayakkara and Dias 2016), are associated with a number of issues that affect their accuracy. Firstly, the tsunami action is typically modelled with an equivalent force according to design prescriptions, without taking into account realistic tsunami inundation time-histories. Current design building codes might be inadequate in assessing tsunami force; in particular, conservative assumptions are typically made for design purposes. Secondly, gross assumptions are made regarding the pressure distribution along the height of the structure resulting from the tsunami actions, without consideration of potential sensitivity of the structural response to variations in the pressure distribution or how the load is discretised and applied to the structural model. Thirdly, available studies typically consider only nonlinear static analyses pushing the structure up to the structural peak strength, where the structure cannot be considered to have failed. It is clear that there is a gap in knowledge in determining how tsunami loads should be applied to a building and which analysis methodology is most suitable for the estimation of building fragility to realistic tsunami.

This paper takes a first step to address these issues by assessing two different nonlinear static analyses and comparing them with dynamic analyses performed considering realistic tsunami inundation time-histories. The assessment is carried out in terms of the ability of each nonlinear static method to predict the peak structural response observed in the dynamic analysis and reproduce the fragility curves for tsunami actions developed from the dynamic analysis. The study takes advantages of the numerical-experimental studies developed at UCL and HR Wallingford for the assessment of tsunami forces on structures (Rossetto et al. 2011; Qi et al. 2014); and extensive tsunami simulations for generating realistic tsunami wave traces (Goda et al. 2015). Two different non-linear static analysis methodologies for the assessment of the building response are defined. The bias induced by adopting pushover analyses is estimated in terms of tsunami fragility curve and recommendations are made as to which nonlinear static analysis is the most suitable for use in the study of building fragility to tsunami.

METHODOLOGY

A case study building selected is a tsunami evacuation building, consisting of 10 storeys and RC frames in both horizontal directions (Figure 1). Building plan dimensions are 36×23 m, with a constant 3.9 m interstorey height for all storeys except for the ground storey, which is 4.5 m high. Six and three bays can be identified along the longitudinal and transverse directions, respectively. The tsunami evacuation building is taken from the design example 3-1 of the "structural design and members section case studies" (Japan Building Disaster Prevention Association 2007). This example structure is designed assuming an earthquake zone coefficient $Z = 1.0$, soil type 2, fundamental vibration period 0.796s, characteristic vibration coefficient $Rt = 0.979$ and base shear coefficient $C_0 = 0.2$. The structure is also designed to resist tsunami loads, assuming a 10 m inundation depth and coefficient a equal to 2.0, yielding an effective inundation equal to 20 m in calculating the wave forces action the building. However, the tsunami design is conducted assuming that the first two floors are "pilotis", i.e. do not have infills. This research study neglects the presence of openings; it is assumed that water flow is obstructed in all bays for the whole height of the structure. Such an assumption causes an increase in tsunami force and allows the investigation of a more common case, where infill walls are installed throughout the height of the structure.
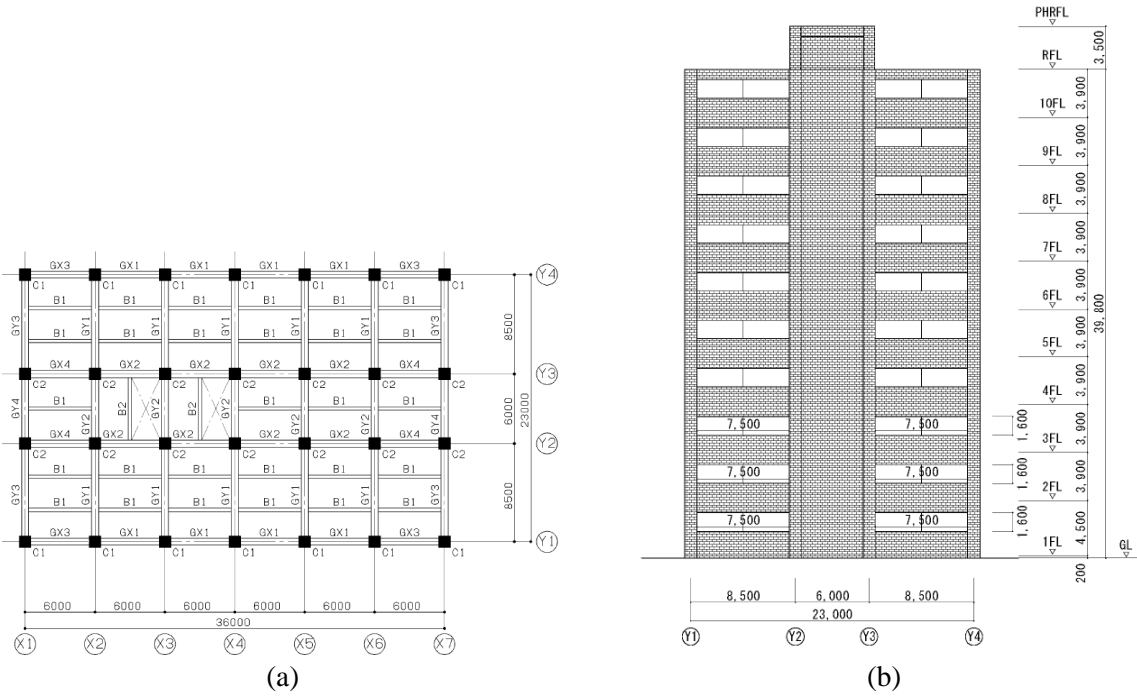
Figure 1. Case study structure: (a) plan view and (b) lateral view (Japan Building Disaster Prevention Association 2007).

Different concrete classes are employed in the design of the structure, with decreasing concrete strength adopted along its height. Two different steel typologies are used for longitudinal and transversal reinforcement, respectively. Column cross-sections assume constant dimensions throughout the building, i.e. 100×100 cm. They are reinforced with a longitudinal reinforcement ratio ranging from 1.32% to 2.25%. Beam cross-section dimensions range from 60×100 cm (at the first floor) to 40×85 cm (at the top floor). Longitudinal reinforcement in beams also varies along the building height, ranging from eight 32 mm-diameter bars at top and bottom flanges (at the first storey) to three 25 mm-diameter bars (at the top floor). 13 mm-diameter stirrups are also adopted in the beams with a spacing ranging from 100 mm to 200 mm. The case study building is modelled in OpenSees (McKenna and Fenves 2013). A 2D model of a transversal frame of the structure is considered. A distributed plasticity approach is adopted for the RC frame model. Each element is modelled with a force-based nonlinear beam-column element, assuming five integration points. Cross-sections are modelled by means of a fibre approach. Three different constitutive laws are defined to model column cross-sections: (a) unconfined concrete is associated to cover fibres; (b) confined concrete is associated to core fibres; and (c) steel material is linked to steel discrete fibres. Further details on the geometry and the modelling of the structure can be found in Petrone et al. (2016).

Tsunami action on the structure is estimated with an equivalent force approach, as suggested in current design guidelines for tsunami resistant structures (FEMA P646 2008): tsunami action on building is modelled through a lateral force, which is caused by the fluid-structure interaction. An existing experimental-analytical research study by (Qi et al. 2014) is employed for this purpose. The study assesses the drag force acting on a rectangular building placed in a free-surface channel flow; the formulation is experimentally validated. Qi et al. (2014) demonstrate that two different flow regimes can occur for a given inlet steady-state flow impacting an obstacle: subcritical and choked. The transition between the two regimes is determined by the Froude number of the impacting flow. As the Froude number increases, a hydraulic jump is observed in downstream of the obstacle and the flow condition turns from subcritical into choked. It is found that the blocking ratio, i.e. the ratio between building width b and flume width w, influences the Froude number threshold between the two regimes. According to (Qi et al. 2014), the tsunami force per unit structural width can be estimated as follows:

$$F/b = sgn(u) \begin{cases} 0.5C_D\rho u^2 h & \text{if } Fr < Fr_c \\ \lambda\rho g^{1/3}u^{4/3}h^{4/3} & \text{if } Fr \geq Fr_c \end{cases} \qquad (1)$$

where $sgn(u)$ is the sign function of the flow velocity, C_D is a drag coefficient, ρ is the density of the fluid assumed $1.20 t/m^3$, u is the flow velocity, h is the inundation depth, λ is the leading coefficient, g is the

acceleration of gravity, and $Fr = u/\sqrt{g \cdot h}$ is the Froude number. The Froude number threshold Fr_c is estimated from Qi et al. (2014):

$$\left(1 - \frac{C_H b}{w}\right)\frac{1}{2Fr_c^{4/3}} + \left(1 - \frac{C_D b}{2w}\right)Fr_c^{2/3} = \left(1 - \frac{C_H b}{w}\right)\frac{1}{2Fr_{d,c}^{4/3}} + Fr_{d,c}^{2/3}; \; Fr_{d,c} = \left(1 - \frac{C_H b}{w}\right)^{1/2} \qquad (2)$$

where C_H is experimentally calibrated to the value of 0.58 and $Fr_{d,c}$ is the Froude number at the back of the building in a critical condition, i.e. when the flow turns into choked. The drag and leading coefficients are a function of the blocking ratio b/w and can be estimated as in Qi et al. (2014), where C_{D0} can be assumed equal to 1.9. Different blocking ratios can be assumed. For this specific study, b/w is set equal to 0.6, considering a dense built environment. Tsunami force F is evaluated assuming a 6 m influence width b, equal to the spacing among transversal frames (Figure 1). The above mentioned formulation allows estimating tsunami force from two input parameters: flow velocity and inundation depth. For a given tsunami inundation flow time-history, the formulation can be applied at each time step in order to assess tsunami force time-history. To avoid discontinuities in force time-histories as the flow state goes from subcritical to choked and vice versa, a smoothing function is proposed to be applied to the $C_D - Fr$ function, as detailed in (Petrone et al. 2016). Qi et al. (2014) focuses on the assessment of net flow force. As the slope of such a pressure distribution is unknown, it is decided to consider two different load patterns representative of extreme cases: (i) a triangular load pattern, which assumes that pressure distributions at the front and at the back are characterised by different slopes with the same water depth; (ii) a trapezoidal load pattern, which assumes that pressure distributions at the front and at the back are characterised by the same slope with different water depths.

Tsunami wave simulation is required in order to assess the impact on the case study structure due to a realistic tsunami. Goda et al. (2015) have generated numerous tsunami wave traces for the 2011 Tohoku tsunami. Tsunami inundation is estimated in terms of inundation depth and flow velocity by evaluating nonlinear shallow water equations considering run-up (Goto et al. 1997). The information on bathymetry, surface roughness, and coastal defence structures is obtained from the Miyagi prefectural government, Japan Hydrographic Association and Geospatial Information Authority of Japan. The bottom friction is evaluated using Manning's formula. Computational cells include those on land, and coastal defence structures are taken into account using an overflowing formula. The initial water displacement caused by earthquake rupture is assessed according to (Okada 1985) and (Tanioka and Satake 1996). Tsunami simulations are performed considering four nested domains (1350-m – 450-m – 150-m – 50-m) and wave-propagation duration of 2 hours with a 0.5s integration time step. Tsunami simulation is performed considering different slip distributions along the fault: the slip distribution by Satake et al. (2013), which was inferred from tsunami waveform data, as well as ten different stochastic realisations of such a slip distribution included in (Goda et al. 2015). Peak inundation depth and flow velocity can be estimated over wide regions, whereas their time-histories are recorded at specific locations. In this study, 73 different locations along the Tohoku coastline are considered for the 11 adopted slip distributions, yielding 803 different tsunami wave traces. Tsunami force can be estimated for each tsunami inundation time-history, according to the above mentioned formulation.

One of the main aims of the study is the assessment of the most reliable method to evaluate fragility curves for tsunami actions. Tsunami structural behaviour can be evaluated by adapting analysis approaches typically used in structural dynamics applications. Here, the case study structure is investigated by means of three different analysis methodologies, features of which are summarised in Table 1:
- Time-history analysis considering actual tsunami onshore flow time-histories (TH)
- Nonlinear static analysis with constant-height load pattern (CHPO)
- Nonlinear static analysis with variable-height load pattern (VHPO)

In TH, a dynamic time-history analysis is carried out considering the tsunami force estimated from simulated time-histories of tsunami onshore flow according to the formulation presented above. The analysis allows the incorporation of the dynamic behaviour of the structure, a feature regarded to be important in the literature but never to date evaluated rigorously. The analysis adopts a transient solver to allow for post-peak behaviour of the structure to be investigated. In particular, once the building's peak strength is reached any increase of force is absorbed in terms of inertia force, which leads the structure to undergo large displacement. Nonlinear static analysis with CHPO assumes a triangular load pattern for a given inundation depth. Similarly to standard pushover analysis, this analysis method increases the roof displacement stepwise and evaluates the magnitude of the load required to attain pre-defined displacement demand levels. This methodology is similar to earthquake pushover analysis (FEMA 273 1997), although it is characterised by a different load pattern. It can be interpreted as an analysis where a constant height load pattern is assumed with a variable flow velocity.

This analysis can be exploited to evaluate structural performance for a given flow velocity (or Froude number) and inundation depth. In particular, a performance point, characterised by the force level corresponding to the assumed IMs, is identified on the pushover curve; such a point yields the predicted response of structure, e.g. interstorey drift demand. VHPO considers a load pattern characterised by a variable height throughout the analysis. At each analysis step the load pattern height is modified according to the assumed inundation depth and the velocity is calculated assuming a constant Froude number. While CHPO is displacement-controlled, i.e. roof displacement is increased step-wise, VHPO is force-controlled. This feature might cause numerical convergence issues in VHPO as, for instance, the inability to capture any degrading branch in the pushover curve.

Table 1. Features of the considered analysis methodologies.

	CHPO	**VHPO**	**TH**
Inundation depth	Constant	Linearly increasing	Actual
Froude number	Increasing	Constant	Actual
Solver	Static	Static	Dynamic
Integrator	Displacement controlled	Force controlled	Newmark

The ability of the different analysis methodologies in predicting the peak response of the structure was investigated in (Petrone et al. 2016). This paper focuses on the identification of the collapse limit state by considering the different analysis methodologies mentioned above. Such a limit state may be attained for either a global failure or a local failure in the structure. Global failures typically refer to plastic mechanisms which involve a variable number of storeys and lead the structure to large displacements, whereas local failure may occur due to shear failure of a single element. Local failure is identified as the attainment of shear capacity in a member according to the formulation proposed by (Biskinis et al. 2004). Different approaches are adopted to detect global failure in the pushover analyses and the time-history analysis. For the pushover analyses, the structure is assumed to be failed when tsunami peak force exceeds structural strength; structural strength is assessed as the peak force in the pushover curve. This definition of collapse implicitly assumes that ductility does not play a role in the structural assessment. For time-history analysis, instead, collapse is estimated from the outcomes of the analysis. It is assumed that collapse is attained when the structure is deformed up to a displacement which is characterised by a 20% internal force reduction.

RESULTS

The different analysis methods are compared in terms of their ability to predict the collapse fragility curves in this section. Both global structural collapse and local shear failure mechanisms are considered. For this comparison, different tsunami IMs are used to represent the tsunami inundation flow. Figure 2 shows the maximum interstorey drift ratio (IDR) obtained in each methodology versus different tsunami IMs. Tsunami IMs that have been adopted in the literature for empirical tsunami fragility function are considered herein, namely, maximum inundation depth, maximum flow velocity, and peak force. The aim of this analysis is to understand which tsunami IM is best suited to represent the structural analysis data in a fragility assessment. The maximum IDR is selected as it is representative of the demand on structural and (some) non-structural elements, and is conventionally used in earthquake engineering to determine structural damage (Rossetto et al. 2016). For clarity of the illustration, it should be noted that in Figure 2 all pushover analyses showing global failure are assigned with an IDR of >0.05 in the plots; this is because all TH analyses exhibiting IDR larger than 0.05 are seen to sustain global failure. It is interesting to note that for the TH analysis results there is a jump in response between IDR equal to 0.015 and 0.050 in Figure 2. This indicates the sudden failure of the structure under tsunami actions for the TH analysis. As the tsunami force exceeds the structural strength, any increase in force is absorbed by inertia and damping forces. Such forces lead the structure to large displacements abruptly. The IM-IDR trends show that peak force is better correlated with IDR than flow velocity and inundation depth (as expected). Inundation depth is not an efficient IM despite the force distribution being significantly influenced by it. Peak force is an efficient IM since failure occurs as soon as it exceeds structural strength and the structural strength is not significantly influenced by specific features of the

tsunami wave trace. Indeed, either 1-storey or 2-storey local mechanism leads to the failure of the structure for all considered tsunami wave traces and the structural strength associated to these mechanisms is included in a narrow range of base shear.
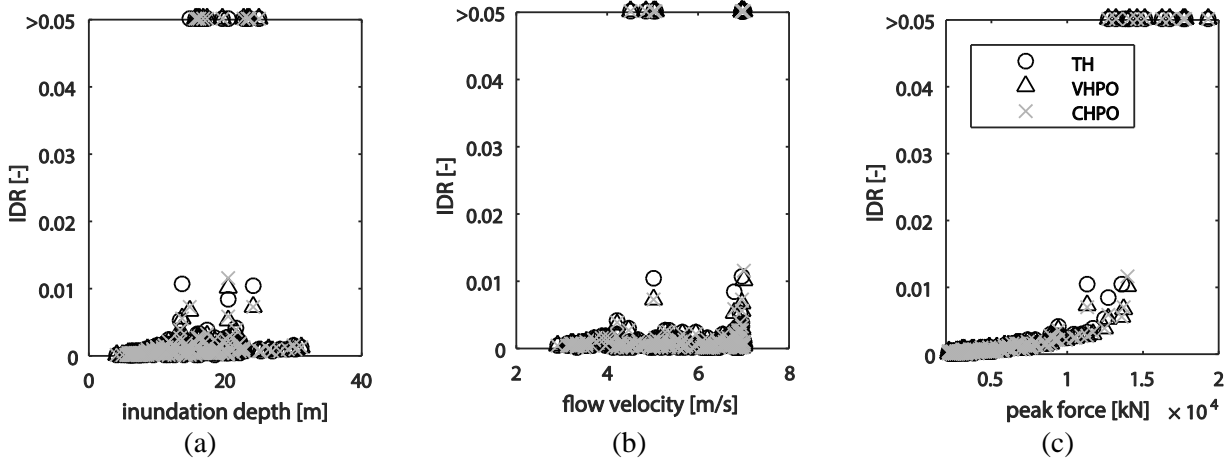

Figure 2. Maximum IDR trend vs different tsunami IMs, assuming a triangular load pattern: (a) inundation depth, (b) flow velocity, and (c) peak force.

The fragility curves yield the probability that the structure has exceeded the collapse limit state for a given IM. The first part of the investigations focuses on fragility curves due to global failures, neglecting the occurrence of shear failure in the elements. Their assessment is performed considering the output of the analysis for each tsunami inundation time-history as a binary variable: 1 and 0 for the collapsed and non-collapsed cases, respectively. A point characterised by the tsunami peak force and the binary variable can be plotted for each analysis (Figure 3). A logistic regression with a probit link of the data points is employed. Figure 3 presents the fragility functions obtained for the three methodologies. In these plots, VHPO is seen to provide a fragility function that closely matches the TH method in the case where a triangular load pattern is adopted. A larger discrepancy of the fragility curves is noticed for the trapezoidal load pattern. Such an agreement confirms that when the peak force of the structure is achieved, the failure is sudden. The mean collapse fragility curves of the CHPO method are slightly shifted with respect to the TH curves, showing a higher fragility. The systematic underestimation of structural strength in CHPO is the main cause of this phenomenon (Petrone et al. 2016).
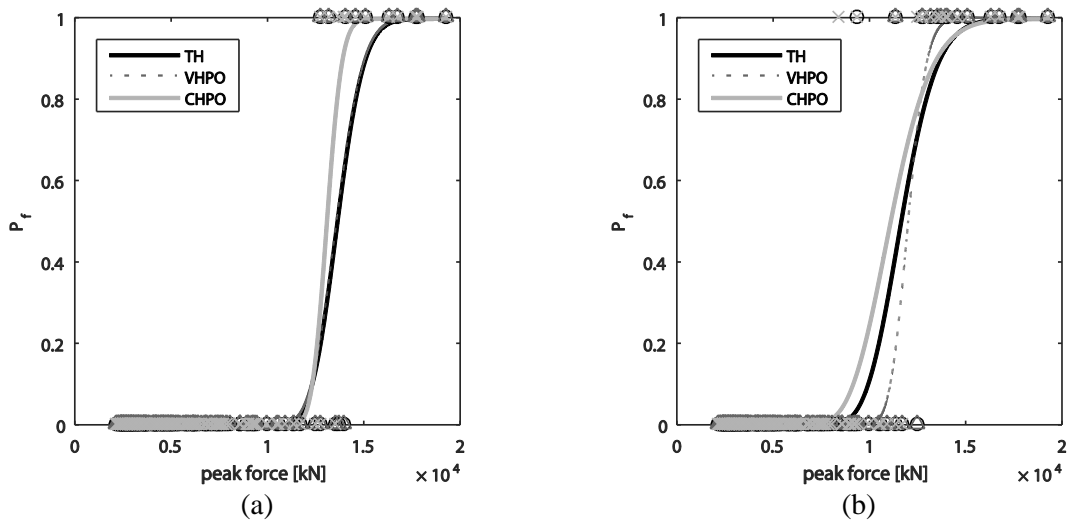

Figure 3. Fragility curves for global failure limit state considering (a) triangular loads and (b) trapezoidal loads.

The collapse of structures may be precipitated by the occurrence of shear failure in key structural elements. In particular, for the adopted structure and load patterns, shear failure in the 1st storey column where tsunami loads are applied always anticipates the failure of the structure. The fragility curves can then be derived

considering local shear failure in addition to global failure for the two different load patterns (Figure 4). VHPO again is seen to provide a close match to the mean collapse fragility curve assessed with TH. Instead, CHPO predicts a lower fragility as a consequence of a shear demand underestimation. From a design perspective, CHPO might give an unsafe-sided estimation of collapse fragility due to shear failure. The use of trapezoidal loads leads to an even lower fragility prediction, contrary to the global failure case. This can be explained by smaller shear demands at the column base due to the load pattern shape. Hence, while trapezoidal load patterns might be more demanding in terms of global failure modes, triangular load patterns typically induce a more severe shear demand on lower storeys of the structure. Comparison of the constructed fragility curves shown in Figure 4 points out that the significant influence due to local shear failure modes may play in fragility assessment. The assessment of this particular structure that has been designed to resist earthquakes and tsunamis to modern Japanese codes suggests that this design code underestimates the shear actions of a tsunami when the effect of infill walls is considered in the force calculation. Moreover, the dispersion in the collapse assessment, denoted by the logarithmic standard deviation of the lognormal distributions, is always lower than 0.20 for the considered structure. This confirms the good efficiency of the peak force, which is able to predict with relatively low uncertainty the occurrence of collapse in a structure subjected to tsunami action.
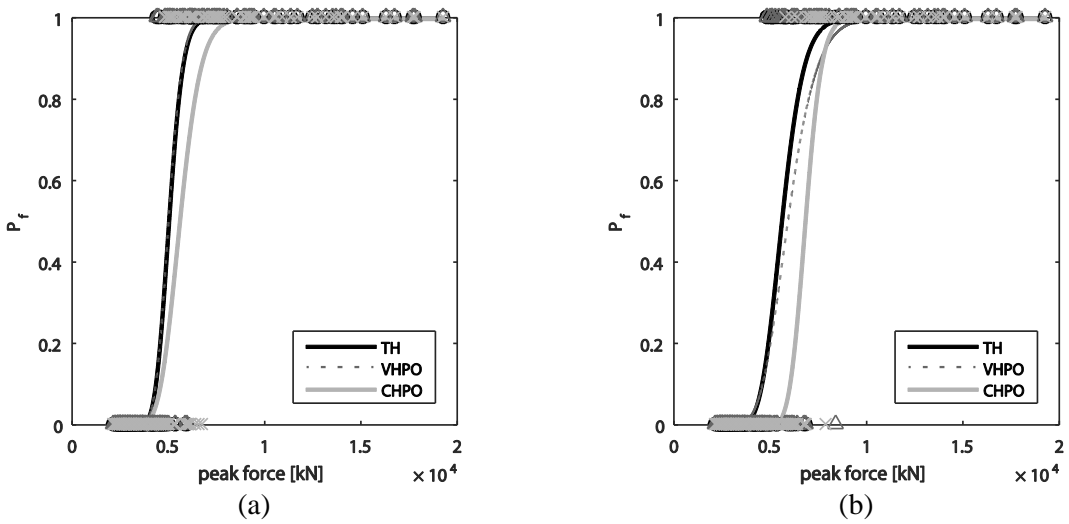

Figure 4. Fragility curves considering shear failure for (a) triangular and (b) trapezoidal loads.

CONCLUSIONS

The paper presents a comparison of different nonlinear static analyses versus dynamic analysis in assessing tsunami impact on buildings. In particular, three different analysis methodologies of constant-height pushover (CHPO), variable-height pushover (VHPO), and time-history (TH) analyses are compared in terms of their abilities to assess collapse fragility curves for tsunami actions. A reinforced concrete frame tsunami evacuation building is selected as a case study for the comparative study and is subjected to the simulated 2011 Tohoku tsunami inundation flows. A tsunami inundation simulation is employed to define a set of tsunami inundation time-histories in terms of inundation depth and flow velocity at different sites in the Tohoku region of Japan. Tsunami force is evaluated according to a recent formulation, which is modified in this study in order to be applicable to a generic tsunami inundation trace. Two different load patterns, i.e. triangular and trapezoidal, are adopted to distribute the tsunami force along the height of the structure.
It is found that VHPO provides a good prediction of the collapse fragility curves obtained from the TH analysis under a wide range of tsunami time-histories. CHPO provides a larger fragility in case global failure is considered and a smaller fragility for local (shear) failure. Such a discrepancy is about 10% in median fragility value. On the basis of these results, it can be concluded that PO methods are a good proxy for TH. In particular, it is recommended that VHPO be used in future fragility analysis of buildings subjected to tsunami. The developed procedure for fragility assessment will be validated through the comparison of analytical fragility curves with empirical fragility curves applied to a portfolio of structures.

ACKNOWLEDGEMENTS

REFERENCES

Biskinis DE, Roupakias GK and Fardis MN. Degradation of shear strength of reinforced concrete members with inelastic cyclic displacements, *ACI Structural Journal*, 2004, 101(6): 773-783.

Charvet I, Ioannou I, Rossetto T, Suppasri A and Imamura F. Empirical fragility assessment of buildings affected by the 2011 Great East Japan tsunami using improved statistical models, *Natural Hazards*, 2014, 73(2): 951-973.

Dias WPS, Yapa HD and Peiris LMN. Tsunami vulnerability functions from field surveys and Monte Carlo simulation, *Civil Engineering and Environmental Systems*, 2009, 26(2): 181-194.

FEMA 273 (1997). *NEHRP guidelines for the seismic rehabilitation of buildings*, Washington, DC.

FEMA P646 (2008). *Guidelines for design of structures for vertical evacuation from tsunamis*, Applied Technology Council, Redwood City, CA, US.

Foytong P, Ruangrassamee A, Lukkunaprasit P and Thanasisathit N. Behaviours of reinforced-concrete building under tsunami loading, *The IES Journal Part A: Civil & Structural Engineering*, 2015, 8(2): 101-110.

Goda K, Yasuda T, Mori N and Mai PM. Variability of tsunami inundation footprints considering stochastic scenarios based on a single rupture model: Application to the 2011 Tohoku earthquake, *Journal of Geophysical Research: Oceans*, 2015, 120(6): 4552-4575.

Goto C, Ogawa Y, Shuto N and Imamura F (1997). *Numerical method of tsunami simulation with the leap-frog scheme (IUGG/IOC Time Project)*, UNESCO, Paris, France.

Japan Building Disaster Prevention Association (2007). *Structural design-member cross-section case studies*, Minister of Land, Infrastructure and Transport specified seismic retrofitting support center. Japan Building Disaster Prevention Association, (in Japanese)

Koshimura S, Oie T, Yanagisawa H and Imamura F. Developing fragility functions for tsunami damage estimation using numerical model and post-tsunami data from Banda Aceh, Indonesia, *Coastal Engineering Journal*, 2009, 51(3): 243-273.

McKenna F and Fenves GL (2013). *OpenSees Manual http://opensees.berkeley.edu*, Pacific Earthquake Engineering Research Center, Berkeley, California.

Nanayakkara KIU and Dias WPS. Fragility curves for structures under tsunami loading, *Natural Hazards*, 2016, 80(1): 471-486.

Okada Y. Surface deformation due to shear and tensile faults in a half-space, *Bulletin of the Seismological Society of America*, 1985, 75(4): 1135-1154.

Park S, van de Lindt JW, Cox D, Gupta R and Aguiniga F. Successive earthquake-tsunami analysis to develop collapse fragilities, *Journal of Earthquake Engineering*, 2012, 16(6): 851-863.

Petrone C, Rossetto T and Goda K. Fragility assessment of a RC structure under tsunami actions via nonlinear static and dynamic analyses, *Engineering Structures*, 2016, (under review).

Qi ZX, Eames I and Johnson ER. Force acting on a square cylinder fixed in a free-surface channel flow, *Journal of Fluid Mechanics*, 2014, 756: 716-727.

Rossetto T, Allsop W, Charvet I and Robinson DI. Physical modelling of tsunami using a new pneumatic wave generator, *Coastal Engineering*, 2011, 58(6): 517-527.

Rossetto T, Gehl P, Minas S, Douglas J, Duffour P and Galasso C. FRACAS: A capacity spectrum approach for seismic fragility assessment including record-to-record variability, *Engineering Structures*, 2016, accepted.

Satake K, Fujii Y, Harada T and Namegaya Y. Time and space distribution of coseismic slip of the 2011 Tohoku earthquake as inferred from tsunami waveform data, *Bulletin of the Seismological Society of America*, 2013, 103(2B): 1473-1492.

Suppasri A, Koshimura S and Imamura F. Developing tsunami fragility curves based on the satellite remote sensing and the numerical modeling of the 2004 Indian Ocean tsunami in Thailand, *Natural Hazards and Earth System Sciences*, 2011, 11(1): 173-189.

Suppasri A, Mas E, Charvet I, Gunasekera R, Imai K, Fukutani Y, Abe Y and Imamura F. Building damage characteristics based on surveyed data and fragility curves of the 2011 Great East Japan tsunami, *Natural Hazards*, 2012, 66(2): 319-341.

Tanioka Y and Satake K. Tsunami generation by horizontal displacement of ocean bottom, *Geophysical Research Letters*, 1996, 23(8): 861-864.